Acta Crystallographica Section B
Structural Science
ISSN 0108-7681

Competing hydrogen-bonding patterns and phase transitions of 1,2-diaminoethane at varied temperature and pressure

Armand Budzianowski, Anna Olejniczak and Andrzej Katrusiak*

Faculty of Crystal Chemistry, Adam Mickiewicz University, Grunwaldzka 6, 60-780 Poznań, Poland

Correspondence e-mail: katran@amu.edu.pl

Received 22 May 2006
Accepted 31 July 2006

1,2-Diaminoethane has been *in-situ* pressure- and temperature-frozen; apart from two known low-temperature phases, Iα and II, three new phases, Iβ, Iγ and III, have been observed and their structures determined by X-ray diffraction. The measurements at 0.1 MPa were carried out at 274, 243 and 224 K, and 296 K measurements were made at 0.15 GPa (phase Iα), at 0.3 and 1.1 GPa (phase Iβ), at 1.5 GPa (phase Iγ), and at 0.2, 0.3 and 0.5 GPa (phase III). All these phases are monoclinic, space group $P2_1/c$, but the unit-cell dimension of phases Iα and III are very different at 296 K: $a_{I\alpha}$ = 5.078 (5), $b_{I\alpha}$ = 7.204 (8), $c_{I\alpha}$ = 5.528 (20) Å, $\beta_{I\alpha}$ = 115.2 (2)° at 0.15 GPa, and a_{III} = 5.10 (3), b_{III} = 5.212 (2), c_{III} = 7.262 (12) Å, β_{III} = 111.6 (4)° at 0.2 GPa, respectively; in both phases Z = 2. An ambient-pressure low-temperature phase II has been observed below 189 K. Discontinuities in the unit-cell dimensions and in the N···N distance mark the isostructural transition between phases Iα and Iβ at 0.2 GPa, which can be attributed to a damping process of the NH_2 group rotations. In phase Iγ the unit-cell parameter a doubles and Z increases to 4. The molecule has inversion symmetry in all the structures determined. 1,2-Diaminoethane can be considered as a simple structural ice analogue, but with NH···N hydrogen bonds and with the H-atom donors (four in one molecule) in excess over H-atom acceptors (two per molecule). Thus, the transformations of 1,2-diaminoethane phases involving the conformational dynamics affect the hydrogen-bonding geometry and molecular association in the crystal. The 1,2-diaminoethane:1,2-dihydroxyethane mixture has been separated by pressure-freezing, and a solid 1,2-diaminoethane crystal in liquid 1,2-dihyroxyethane has been obtained.

1. Introduction

1,2-Diaminoethane (ethylene diamine, ethane-1,2-diamine, $C_2H_8N_2$) is the simplest of the α,ω-diaminoalkanes (Fig. 1) and it is used in the production of carbamate fungicides, surfactant, dyes, chelating agents *etc.* Its melting point is 284.29 K (Messerly *et al.*, 1975). Thermal analyses of this compound showed that there is a solid-state phase transition at *ca* 201 K (Jamet-Delcroix, 1973). Jamet-Delcroix obtained a single crystal of 1,2-diaminoethane at 213 K, the temperature chosen to avoid destruction of the single-crystal sample by the solid-state phase transition. The crystal structure was determined by an X-ray diffraction study carried out by photographic techniques; the crystal was monoclinic, space group $P2_1/c$, with a = 5.65 (5), b = 7.14 (2), c = 5.50 (5) Å, β = 125.6 (7)°. A precise temperature, of 189 K, of the solid-state phase transition in 1,2-diaminoethane was measured by adiabatic calorimetry by Messerly *et al.* (1975). Although Jamet-Delcroix observed

destruction of the 1,2-diaminoethane single crystals cooled below this phase transition, Thalladi *et al.* (2000) succeeded in cooling a single-crystal sample to 130 K and determined its structure. Thalladi *et al.* (2000) referred to the work of Jamet-Delcroix (1973), but they described their structure in a different unit-cell setting and hence reported different unit-cell dimensions without comments; they also mentioned that the differential scanning calorimetry analysis showed no sign of a phase transition in 1,2-diaminoethane down to 130 K. The reported crystal structure at 130 K was monoclinic, space group $P2_1/c$, with lattice constants $a = 5.047$ (2), $b = 7.155$ (2), $c = 5.475$ (2) Å, $\beta = 115.36$ (3)°. The unit-cell setting applied by Jamet-Delcroix (1973) at 213 K can be transformed to that used by Thalladi *et al.* (2000) at 130 K by choosing another **a** direction, according to the matrix

$$\begin{pmatrix} a \\ b \\ c \end{pmatrix}_{\mathrm{T}} = \begin{pmatrix} 1 & 0 & 1 \\ 0 & -1 & 0 \\ 0 & 0 & -1 \end{pmatrix} \cdot \begin{pmatrix} a \\ b \\ c \end{pmatrix}_{\mathrm{JD}} \qquad (1)$$

where subscripts JD and T indicate the unit-cell assignments by Jamet-Delcroix (1973) and Thalladi *et al.* (2000), respectively. Thus, in the light of the calorimetric studies by Jamet-Delcroix (1973) demonstrating the existence of a phase transition around 201 K [this temperature later refined to 189 K by Messerly *et al.* (1975)] and according to our results confirming the solid-state phase transition about 189 K, the structural determination by Thalladi *et al.* (2000) was performed on a supercooled crystal.

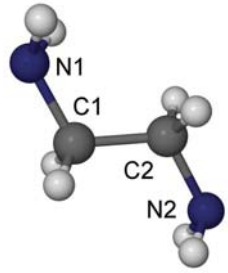

Figure 1
Ball and stick representation of the 1,2-diaminoethane molecule.

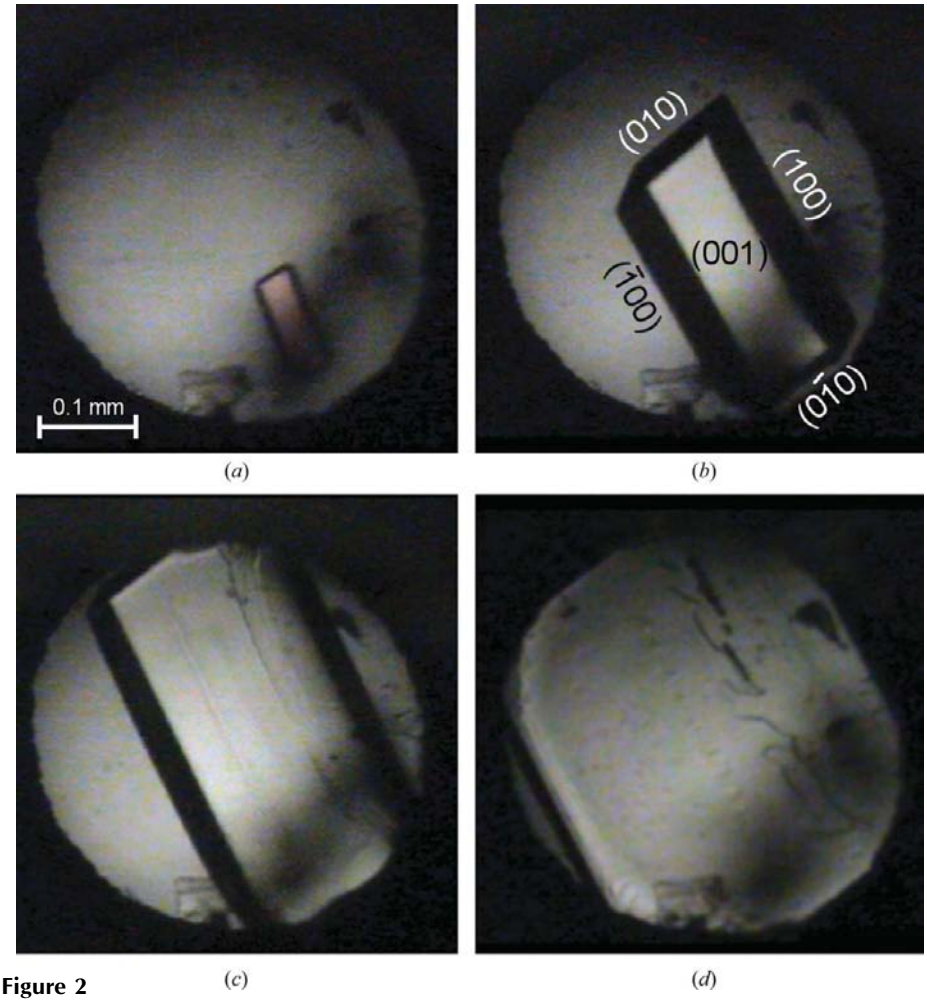

Figure 2
1,2-Diaminoethane in phase III – several stages of the single-crystal growth in the high-pressure chamber: the single-crystal grain at (*a*) 383 K, (*b*) 353 K, with Miller indices of the crystal faces indicated, and (*c*) 323 K; (*d*) the crystal almost completely filling the chamber, when pressure stabilized to 0.3 GPa at 296 K. A small ruby chip for pressure calibration is visible at the bottom of the chamber in this photograph.

The dimensions of the unit cell measured by Jamet-Delcroix (1973) at 213 K and transformed according to (1) are $a = 5.10$ (7), $b = 7.14$ (2), $c = 5.50$ (5) Å, $\beta = 115.7$ (7)°. This unit-cell setting, consistent with that assigned by Thalladi *et al.* (2000), will be used below, because its β angle is smaller than that in the setting introduced by Jamet-Delcroix (1973). Thus, the same phase of 1,2-diaminoethane, denoted as phase I by Messerly *et al.* (1975) and as phase Iα in the text below, was determined in those two structural studies.

The main purpose of the present study on 1,2-diaminoethane was to investigate the molecular association and the hydrogen-bonding pattern in this simple NH···N-bonded molecular compound. The 1,2-diaminoethane molecule has four H-atom donor and two H-atom acceptor sites. Thus, in principle, one molecule can form four NH···N hydrogen bonds. The role of the remaining two amino H atoms for molecular association is not clear. The NH_2 group can dynamically rotate about the C—N bond and the H atoms involved in the hydrogen bonding can exchange with those not involved. Such behaviour in certain respects resembles the structures of H_2O ice Ih, where the water molecules are orientationally disordered

but the numbers of hydrogen-bond donors and acceptors are equal. H_2O ice is well known for its rich phase diagram, and it was intended to check if analogous polymorphic transformations occurred in $C_2H_8N_2$. It was hoped that the excess hydrogen-bond donors in 1,2-diaminoethane would make the relationships between hydrogen-bond structure and crystal properties more apparent than in H_2O ice. On the other hand, the properties of the NH···N-bonded structure are of particular interest in relation to the ferroelectricity recently observed in 1,4-diazabicyclo[2.2.2]octane (denoted dabco) NH^+···N-bonded complexes (Katrusiak & Szafrański, 1999; Szafrański *et al.*, 2002). It was found that the NH^+···N hydrogen bonds resemble short OH···O hydrogen bonds in some way. However, the crystal structure of the NH^+···N-bonded ferroelectrics are simpler than their OH···O analogues in this respect: the NH^+···N-bonded dabco aggregates are linear, whereas the OH···O bonds form zigzag-like patterns. Moreover, it was found most recently that the transformation of the NH^+···N bonds in the dabco ferroelectrics leads to their relaxor-like behaviour (Szafrański & Katrusiak, 2004), and that the NH^+···N-bonded aggregates in dabco·HBr can be regarded as a one-dimensional ice model, because the disorder of protons persists to low temperatures (Budzianowski & Katrusiak, 2006*a*).

The NH···N bonds between neutral 1,2-diaminoethane molecules are weaker than NH^+···N bonds in dabco complexes. Because of the excess of H-atom donors over acceptors in 1,2-diaminoethane, not only H-atom exchanges between hydrogen-bonded NH_2 groups, analogous to those in ice, but also H-atom exchanges between hydrogen-bonded and non-bonded sites can take place. 1,2-Diaminoethane can also be regarded as a fragment of the dabco molecule, where the ethylene $-CH_2-CH_2-$ bridges are in the *s-trans* conformation (or close to it) (N—C—C—N angle within $\pm 20^\circ$). To study the possible transformations of 1,2-diaminoethane we have varied the thermodynamic conditions of pressure and temperature and determined the *in-situ* frozen and transformed crystal structures by single-crystal X-ray diffraction.

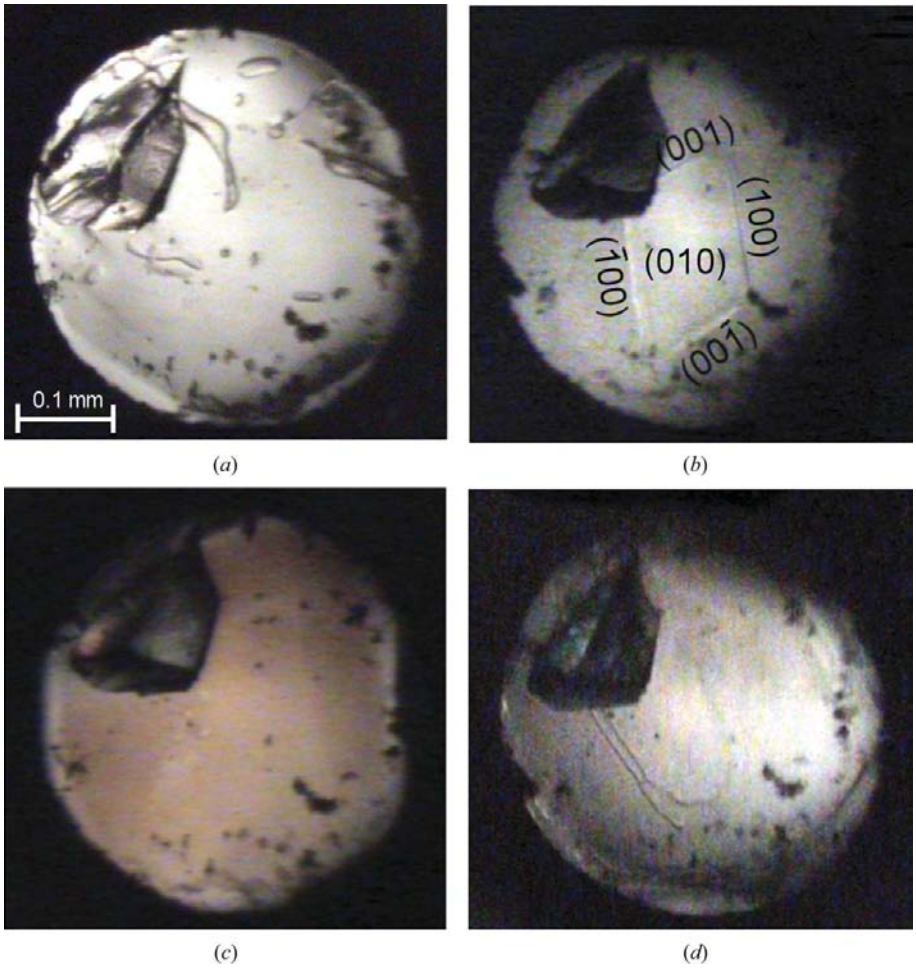

Figure 3
1,2-Diaminoethane in phase Iβ: (*a*) one single crystal filling the pressure chamber at 1.1 GPa and 296 K; (*b*) the DAC heated to 423 K with one single-crystal plate left; (*c*) the single-crystal plate grown to the edges of the chamber after increased pressure; and (*d*) the single-crystal filling the whole volume of the chamber, when pressure stabilized to 1.5 GPa at 296 K. Miller indices of the crystal faces are indicated in photograph (*b*). A large (0.1 mm) ruby chip for pressure calibration is placed in the upper-left part of the chamber.

2. Experimental

1,2-Diaminoethane was pressure frozen *in situ* in a modified Merrill–Bassett miniature diamond–anvil cell (DAC), made in our workshop. The freezing pressure of 0.15 (5) GPa at 296 K was determined when the polycrystalline sample and liquid coexisted in the DAC. The pressure was then further increased to 0.30 (5) GPa, and the DAC was heated till all crystals except one melted, after which the DAC was cooled slowly allowing this one grain to grow up to 296 K (Fig. 2). Diffraction data were measured for this single crystal. Next, the DAC was loaded again and the pressure increased to 1.1 GPa (Fig. 3*a*). After collecting the diffraction data the crystal was heated again, and when one small grain was left the pressure in the DAC was increased (Fig. 3*b*). By slowly cooling the DAC, a single crystal at 1.5 GPa was obtained (Figs. 3*c* and 3*d*). When this diffraction-data measurement was completed, the pressure was decreased to 0.3 GPa and the measurement repeated. In another experiment the DAC was loaded with 1,2-diaminoethane, but an air bubble was left when sealing the DAC chamber to

ensure low-pressure conditions. The DAC was then cooled till 1,2-diaminoethane froze in a polycrystalline form. By gently warming the DAC, a single-crystal grain was obtained; the DAC chamber was slowly squeezed to 0.2 GPa, while the temperature was increased to 296 K, allowing this one grain to grow. After collecting data the pressure was further increased and the crystal was remeasured at 0.5 GPa. When the pressure was increased to 0.7 GPa, the crystal shattered. The DAC chamber was heated again till one small grain remained and the single crystal was grown by slowly cooling the DAC. After 24 h the pressure in the DAC decreased to 0.45 GPa and after one week it decreased to 0.15 GPa. The diffraction data were then measured.

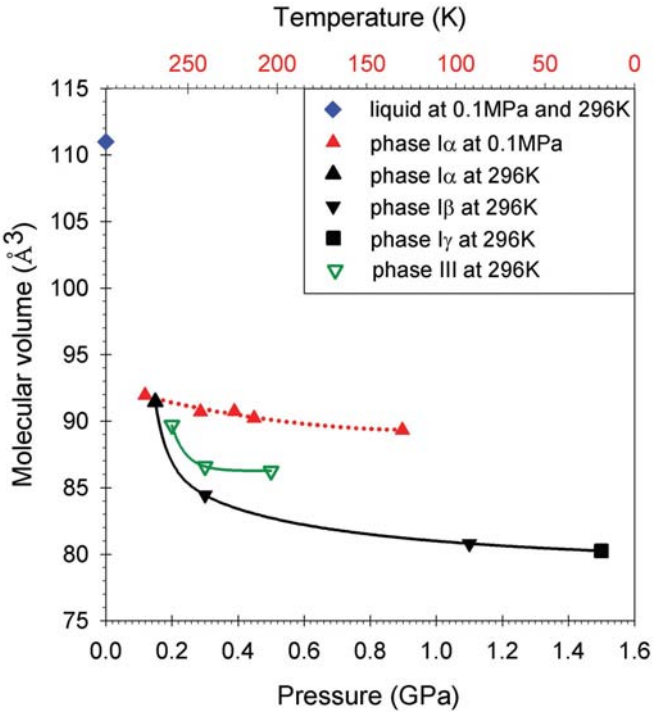

Figure 4
Molecular volume of 1,2-diaminoethane as a function of pressure at 296 K (the scale at the bottom, solid lines) and as a function of temperature at 0.1 MPa (the reversed scale at the top, dotted lines). The lines joining the points have been drawn only for guiding the eye.

Our X-ray diffraction experiments showed that 1,2-diaminoethane forms a series of phases. Phase Iα cooled below 189 K transforms to phase II (Messerly *et al.*, 1975), and when pressurized phase Iα transforms to phases denoted Iβ and Iγ. By pressure-freezing, another phase, III, was formed. Phases Iβ and Iγ were always obtained from phase Iα, and their unit-cell dimensions and structures are closely related. Therefore, Greek letters have been used for denoting these phases and for distinguishing them from the very different phases II and III. The crystal habits of phases Iα and III are clearly different. Phase Iα can be obtained by cooling 1,2-diaminoethane, in or outside the DAC, at atmospheric pressure, while phase III can be obtained by increasing the pressure at room or higher temperature. The diffraction data showed that phase III was stable to *ca* 0.5 GPa. When the high-pressure chamber was further squeezed and the pressure increased, a transformation of phase III to phase Iβ was observed. It can be seen in Fig. 4 that the molecular volume V_m of phase III is lower than that of phase Iα, but larger than that of phase Iβ at corresponding pressures. Thus, phase III is more favoured than phase Iα at lower pressures, but phase Iβ is more favoured than phase III at pressures above 0.5 GPa. The transformation of phase III into Iβ results from this interdependence. Because the transformation of phase III took place at isochoric conditions in the DAC, this transfor-

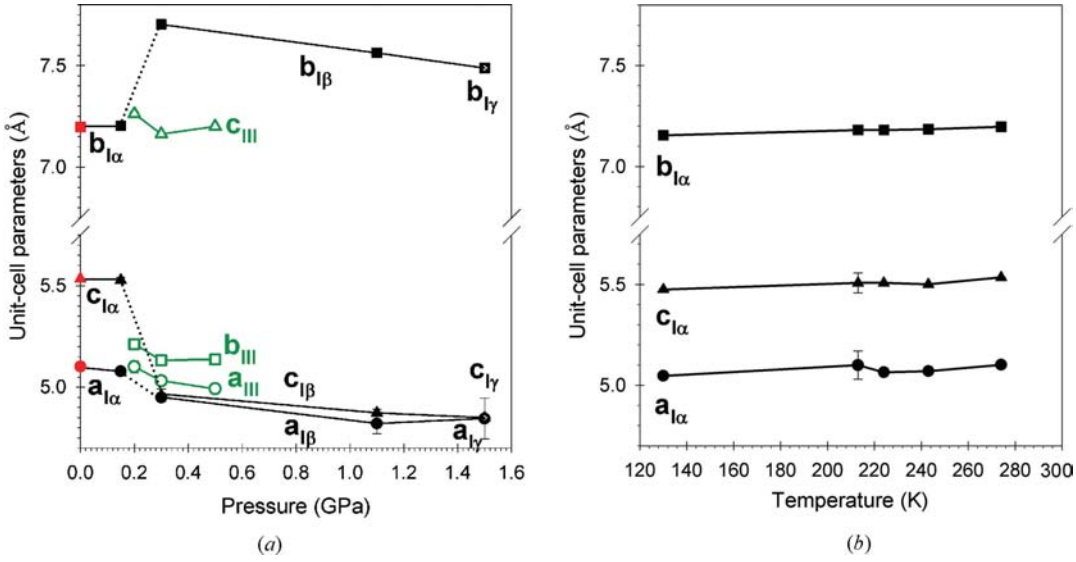

Figure 5
Unit-cell dimensions of 1,2-diaminoethane crystalline phases plotted as a function of (*a*) pressure at 296 K and (*b*) temperature at 0.1 MPa for phases Iα, Iβ, Iγ and III: $a_{I\alpha}$, $a_{I\beta}$, $a_{I\gamma}$ (black circles); $b_{I\alpha}$, $b_{I\beta}$, $b_{I\gamma}$ (black squares); $c_{I\alpha}$, $c_{I\beta}$, $c_{I\gamma}$ (black triangles); a_{III} (green open circles); b_{III} (green open squares); c_{III} (green open triangles). For phase Iγ the $a_{I\gamma}/2$ value has been plotted for convenient comparison with other phases. The red points at 0.1 MPa are determined at 274 K. The lines joining the points have been drawn as a guide to the eye. The unit-cell dimensions measured at 213 K by Jamet-Delcroix (1973) and in the metastable region at 130 K by Thalladi *et al.* (2000) have been included.

mation decreased pressure in the chamber (V_m in phase Iβ is smaller than in phase III at corresponding pressures – see Fig. 4). The transformation of phase III to phase Iα in the whole volume of the pressure chamber decreased the pressure to 0.15 GPa, at which the structure of phase Iα was determined. The diffraction measurements were usually carried out hours or even days after freezing the 1,2-diaminoethane samples or increasing their pressure, in order to minimize the possibility of measuring metastable phases.

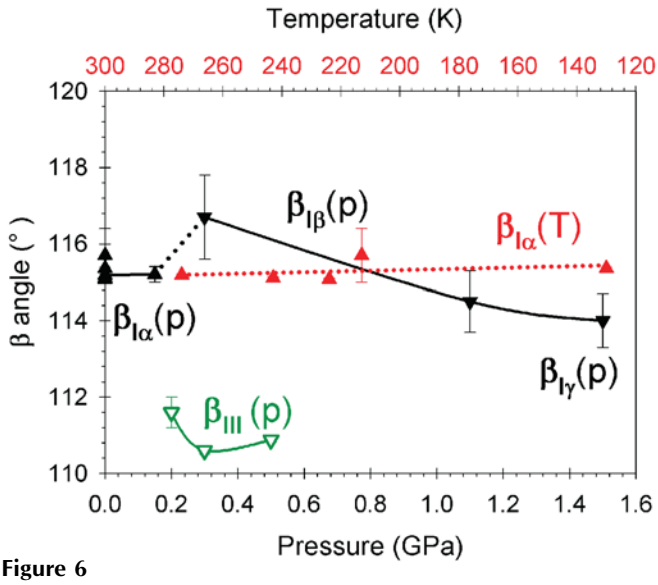

Figure 6
Unit-cell angle β of 1,2-diaminoethane crystalline phases plotted as a function of temperature at 0.1 MPa (the reverse scale above the plot) for the temperature-frozen phase Iα (red down-triangles), and pressure at 296 K (the scale at the bottom) for phases Iα, Iβ and Iγ (black up-triangles) and phase III (green open down-triangles). The lines joining the points have been drawn as a guide to the eye. Where not indicated, the error bars are smaller than the symbols used.

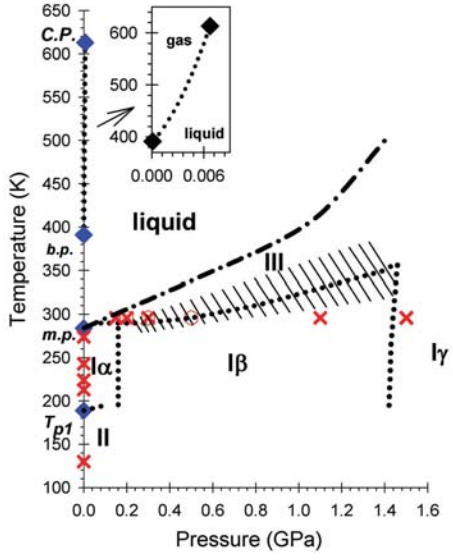

Figure 7
Proposed phase diagram of 1,2-diaminoethane. *C.P.* denotes the critical point at 0.067 GPa and 613.3 K (Wilson *et al.*, 1996); *b.p.* the boiling point at 0.1 MPa and 391.2 K (Sigma–Aldrich, 2005); *m.p.* the melting point at 0.1 MPa and 284 K (Messerly *et al.*, 1975); and T_{p1} the temperature of the solid–solid phase transition at atmospheric pressure and 189 K (Messerly *et al.*, 1975). The red crosses and hexagons show the thermodynamic coordinates of the known crystallographic structures. The dotted lines indicate phase boundaries and the dashed area indicates metastable regions between phases Iβ and III; the dot–dash line is the melting curve.

The distinction between phases Iα and Iβ has been mainly based on pressure dependence of the unit-cell parameters (Figs. 5 and 6), and on clearly anomalous compression of the N···N distances in the Iα and Iβ structures (discussed below). Phase Iγ is distinguished by the observed new reflections doubling the cell volume, although these new reflections were very weak.

The visual observation of the freezing process, crystal habits and transformations between the phases, as well as the crystal data, allowed a phase diagram of 1,2-diaminoethane to be outlined, as shown in Fig. 7. Apart from the phases indicated in this phase diagram we also made observations of other phases – most probably metastable ones – which appeared on temperature- or pressure-freezing of 1,2-diaminoethane, and were distinguishable by morphology (for example, long thin needles). These metastable crystals dissolved when crystals of phase Iα or III grew in the DAC. The process of freezing liquids is very convenient for observations in the DAC, as pressure and temperature can be controlled simultaneously.

After this series of high-pressure experiments, the study of 1,2-diaminoethane freezing continued under ambient-pressure and low-temperature conditions. *In-situ* temperature-freezing of 1,2-diaminoethane was performed using a 0.3 mm glass capillary, half-filled with the liquid and closed at both ends. The capillary was mounted on the diffractometer and cooled in a stream of gaseous nitrogen from an Oxford Cryostream attachment. When the temperature decreased, the initial contraction of the liquid and subsequent formation of several small crystals could be observed. One of these crystals was shifted into the X-ray beam along the goniometer-head z-translation before performing the single-crystal diffraction study.

The single-crystal diffraction data were measured at 274, 243 and 224 K and all these structures were determined to be in phase Iα. The crystal was then further cooled below 189 K. Although the crystal was clearly visible in the capillary, the single-crystal diffraction pattern disappeared, and only powder diffraction rings could be observed. This powder diffraction pattern remained practically unchanged at 130 and 97 K. This single-crystal destruction strongly corroborates the report by Jamet-Delcroix (1973) about the first-order destructive phase transition around 201 K [precisely determined by Messerly *et al.* (1975) at 189 K]. The powder diffraction patterns recorded at 0.1 MPa below 189 K could not be indexed according to the structures of phases Iα, Iβ, Iγ or III, which shows that yet another phase, denoted phase II by Messerly *et al.* (1975), exists.

The pressure inside the DAC was calibrated by the ruby-fluorescence method (Piermarini *et al.*, 1975; Mao *et al.*, 1985), using a Betsa PRL spectrometer, with an accuracy of 0.05 GPa. The single-crystal X-ray diffraction studies were carried out with a Kuma KM-4 CCD diffractometer. The

Table 1
High-pressure crystal data and structure refinements details for 1,2-diaminoethane in phases Iα, Iβ, Iγ and III.

	Iα at 0.15 GPa	Iβ at 0.3 GPa	Iβ at 1.1 GPa	Iγ at 1.5 GPa	III at 0.2 GPa	III at 0.3 GPa	III at 0.5 GPa
Crystal data							
Chemical formula	$C_2H_8N_2$	$C_2H_8N_2$	$C_2H_8N_2$	$C_2H_8N_2$	$C_2H_8N_2$	$C_2H_8N_2$	$C_2H_8N_2$
M_r	60.10	60.10	60.10	60.10	60.10	60.10	60.10
Cell setting, space group	Monoclinic, $P2_1/c$	Monoclinic, $P2_1/c$	Monoclinic, $P2_1/c$	Monoclinic, $P2_1/c$	Monoclinic, $P2_1/c$	Monoclinic, $P2_1/c$	Monoclinic, $P2_1/c$
Pressure (GPa)	0.15 (5)	0.30 (5)	1.10 (5)	1.50 (5)	0.20 (5)	0.30 (5)	0.50 (5)
Temperature (K)	296 (2)	296 (2)	296 (2)	296 (2)	296 (2)	296 (2)	296 (2)
a (Å)	5.078 (5)	4.949 (6)	4.82 (5)	9.69 (10)	5.10 (3)	5.031 (10)	4.9921 (18)
b (Å)	7.204 (8)	7.704 (8)	7.563 (5)	7.488 (5)	5.212 (2)	5.132 (3)	5.137 (4)
c (Å)	5.528 (12)	4.96 (3)	4.873 (18)	4.849 (14)	7.262 (12)	7.167 (5)	7.200 (4)
β (°)	115.24 (18)	116.7 (11)	114.5 (8)	114.0 (7)	111.6 (4)	110.60 (12)	110.87 (5)
V (Å^3)	182.9 (6)	169.0 (19)	162 (2)	321 (4)	179.5 (12)	173.2 (4)	172.53 (19)
Z	2	2	2	4	2	2	2
D_x (Mg m^{-3})	1.091	1.182	1.236	1.243	1.113	1.152	1.157
Radiation type	Mo $K\alpha$	Mo $K\alpha$	Mo $K\alpha$	Mo $K\alpha$	Mo $K\alpha$	Mo $K\alpha$	Mo $K\alpha$
μ (mm^{-1})	0.07	0.08	0.08	0.08	0.08	0.08	0.08
Crystal form, colour	Disk, colourless	Disk, colourless	Disk, colourless	Disk, colourless	Disk, colourless	Disk, colourless	Disk, colourless
Crystal size (mm)	0.30 × 0.30 × 0.08	0.42 × 0.42 × 0.10	0.41 × 0.41 × 0.09	0.41 × 0.41 × 0.08	0.42 × 0.42 × 0.11	0.40 × 0.40 × 0.09	0.35 × 0.35 × 0.08
Data collection							
Diffractometer	Kuma KM-4 CCD κ geometry	Kuma KM-4 CCD κ geometry	Kuma KM-4 CCD κ geometry	Kuma KM-4 CCD κ geometry	Kuma KM-4 CCD κ geometry	Kuma KM-4 CCD κ geometry	Kuma KM-4 CCD κ geometry
Data collection method	ω scans	ω scans	ω scans	ω scans	ω scans	ω scans	ω scans
Absorption correction	Integration	Integration	Integration	Integration	Integration	Integration	Integration
T_{min}	0.44	0.48	0.45	0.45	0.47	0.55	0.49
T_{max}	0.84	0.94	0.93	0.93	0.89	0.91	0.82
No. of measured, independent and observed reflections	1259, 224, 188	1260, 117, 113	1159, 124, 103	2437, 235, 225	1272, 141, 125	897, 96, 72	1110, 206, 193
Criterion for observed reflections	$I > 2\sigma(I)$	$I > 2\sigma(I)$	$I > 2\sigma(I)$	$I > 2\sigma(I)$	$I > 2\sigma(I)$	$I > 2\sigma(I)$	$I > 2\sigma(I)$
R_{int}	0.075	0.062	0.064	0.108	0.097	0.091	0.063
θ_{max} (°)	29.6	28.9	29.4	29.8	29.3	29.4	29.9
Refinement							
Refinement on	F^2	F^2	F^2	F^2	F^2	F^2	F^2
$R[F^2 > 2\sigma(F^2)]$, $wR(F^2)$, S	0.084, 0.130, 1.25	0.142, 0.266, 1.76	0.064, 0.212, 0.96	0.237, 0.433, 1.39	0.055, 0.104, 1.10	0.074, 0.253, 1.22	0.059, 0.149, 1.07
No. of reflections	224	117	124	235	141	96	206
No. of parameters	25	20	25	26	25	20	25
H-atom treatment	Constrained to parent site	Constrained to parent site	Constrained to parent site	Constrained to parent site	Constrained to parent site	Constrained to parent site	Constrained to parent site
Weighting scheme	$w = 1/[\sigma^2(F_o^2) + 0.1653P]$, where $P = (F_o^2 + 2F_c^2)/3$	$w = 1/[\sigma^2(F_o^2) + (0.05P)^2 + 0.3P]$, where $P = (F_o^2 + 2F_c^2)/3$	$w = 1/[\sigma^2(F_o^2) + (0.1176P)^2 + 0.1743P]$, where $P = (F_o^2 + 2F_c^2)/3$	$w = 1/[\sigma^2(F_o^2) + (0.05P)^2 + 5P]$, where $P = (F_o^2 + 2F_c^2)/3$	$w = 1/[\sigma^2(F_o^2) + (0.0185P)^2 + 0.1484P]$, where $P = (F_o^2 + 2F_c^2)/3$	$w = 1/[\sigma^2(F_o^2) + (0.1848P)^2]$, where $P = (F_o^2 + 2F_c^2)/3$	$w = 1/[\sigma^2(F_o^2) + (0.0578P)^2 + 0.1608P]$, where $P = (F_o^2 + 2F_c^2)/3$
$(\Delta/\sigma)_{max}$	<0.0001	<0.0001	<0.0001	<0.0001	<0.0001	<0.0001	<0.0001
$\Delta\rho_{max}$, $\Delta\rho_{min}$ (e Å^{-3})	0.10, −0.11	0.12, −0.13	0.10, −0.10	0.33, −0.27	0.10, −0.09	0.15, −0.14	0.13, −0.15
Extinction method	*SHELXL*97	*SHELXL*97	*SHELXL*97	*SHELXL*97	*SHELXL*97	*SHELXL*97	*SHELXL*97
Extinction coefficient	1.00 (13)	0.3 (2)	1.0 (6)	0.8 (3)	10.4 (13)	0.3 (4)	0.3 (2)

Computer programs used: *CrysAlis* (Oxford Diffraction, 2002), *SHELXS97* (Sheldrick, 1990), *SHELXL97* (Sheldrick, 1997), *X-SEED* (Barbour, 2001), *POV-Ray* (Persistence of Vision, 2004).

Table 2
Low-temperature crystal data and structure refinements for 1,2-diaminoethane in phase Iα at 0.1 MPa.

	Iα at 224 K	Iα at 243 K	Iα at 274 K
Crystal data			
Chemical formula	$C_2H_8N_2$	$C_2H_8N_2$	$C_2H_8N_2$
M_r	60.10	60.10	60.10
Cell setting, space group	Monoclinic, $P2_1/c$	Monoclinic, $P2_1/c$	Monoclinic, $P2_1/c$
Temperature (K)	224 (2)	243 (2)	274 (2)
a (Å)	5.065 (1)	5.070 (1)	5.102 (1)
b (Å)	7.181 (1)	7.185 (1)	7.197 (1)
c (Å)	5.508 (1)	5.501 (1)	5.535 (1)
β (°)	115.07 (3)	115.11 (3)	115.18 (3)
V (Å^3)	181.46 (7)	181.45 (7)	183.93 (7)
Z	2	2	2
D_x (Mg m^{-3})	1.100	1.100	1.085
Radiation type	Mo $K\alpha$	Mo $K\alpha$	Mo $K\alpha$
μ (mm^{-1})	0.07	0.07	0.07
Crystal form, colour	Plate, colourless	Plate, colourless	Plate, colourless
Crystal size (mm)	0.6 × 0.4 × 0.1	0.6 × 0.4 × 0.1	0.6 × 0.4 × 0.1
Data collection			
Diffractometer	Kuma KM-4 CCD κ geometry	Kuma KM-4 CCD κ geometry	Kuma KM-4 CCD κ geometry
Data collection method	ω scans	ω scans	ω scans
Absorption correction	None	None	None
No. of measured, independent and observed reflections	1070, 457, 369	1241, 458, 406	940, 452, 330
Criterion for observed reflections	$I > 2\sigma(I)$	$I > 2\sigma(I)$	$I > 2\sigma(I)$
R_{int}	0.061	0.048	0.129
θ_{max} (°)	29.1	29.1	28.6
Refinement			
Refinement on	F^2	F^2	F^2
$R[F^2 > 2\sigma(F^2)]$, $wR(F^2)$, S	0.045, 0.132, 1.11	0.040, 0.112, 1.10	0.085, 0.210, 1.03
No. of reflections	457	458	452
No. of parameters	25	25	25
H-atom treatment	Constrained to parent site	Constrained to parent site	Constrained to parent site
Weighting scheme	$w = 1/[\sigma^2(F_o^2) + (0.0726P)^2 + 0.0014P]$, where $P = (F_o^2 + 2F_c^2)/3$	$w = 1/[\sigma^2(F_o^2) + (0.059P)^2 + 0.0216P]$, where $P = (F_o^2 + 2F_c^2)/3$	$w = 1/[\sigma^2(F_o^2) + (0.1384P)^2]$, where $P = (F_o^2 + 2F_c^2)/3$
$(\Delta/\sigma)_{max}$	<0.0001	<0.0001	<0.0001
$\Delta\rho_{max}$, $\Delta\rho_{min}$ (e Å^{-3})	0.31, −0.16	0.34, −0.15	0.35, −0.29
Extinction method	*SHELXL*97	*SHELXL*97	*SHELXL*97
Extinction coefficient	0.33 (14)	0.38 (11)	0.6 (3)

CrysAlis software (Version 1.171.24; Oxford Diffraction, 2002) was used for the data collection (Budzianowski & Katrusiak, 2004) and the preliminary reduction of the data. After the intensities were corrected for the effects of DAC absorption, sample shadowing by the gasket and the sample absorption (Katrusiak, 2003, 2004), the diamond reflections were eliminated. The systematic absences unequivocally showed that the

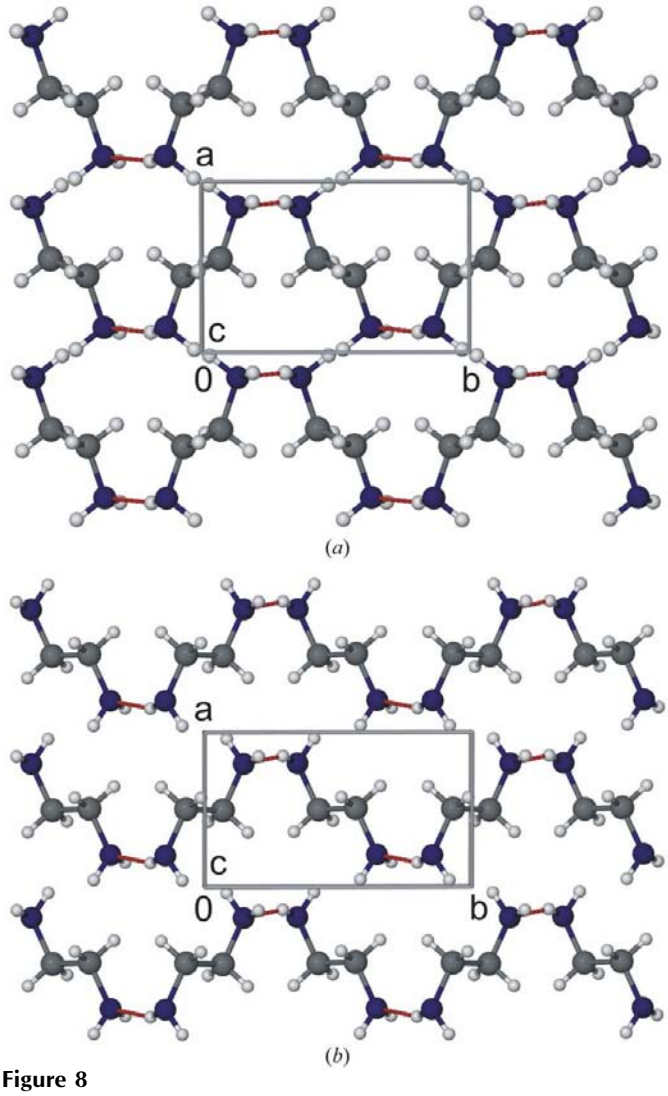

Figure 8
Crystal structure of 1,2-diaminoethane in phases Iα (*a*) and Iβ (*b*) viewed along the sheets shown in Fig. 9(*a*). The criterion of the two shortest hydrogen bonds has been applied for distinguishing these sheets (see Table 3). The hydrogen bonds are represented as red lines.

crystals are monoclinic in space group $P2_1/c$. The unit-cell dimensions have been accounted for the effect of gasket shadowing (Katrusiak, 2006). All structures were solved by direct methods (Sheldrick, 1990) and refined by full-matrix least squares (Sheldrick, 1997). Anisotropic displacement parameters were generally applied for C and N atoms, but for the atoms for which the refinement resulted in non-positive definite ellipsoids the isotropic displacement parameters were retained. The H-atom positions were calculated from molecular geometry after each cycle of the refinement (C—H = 0.97 Å) and U_{iso} values of amino H atoms were constrained to $1.2U_{eq}$ of the carrier atoms, except in the structure at 1.5 GPa, for which all H atoms were constrained to $1.2U_{iso}$ of the carrier atoms. The crystal data and the structure refinement details are listed in Tables 1 and 2.[1] Structural drawings were

[1] Supplementary data for this paper are available from the IUCr electronic archives (Reference: AV5066). Services for accessing these data are described at the back of the journal.

Table 3
Shortest intermolecular N···N and N···H distances (Å) in phases Iα, Iβ, Iγ and III.

The values at 213 and 130 K are calculated from structures determined by Jamet-Delcroix (1973) and Thalladi *et al.* (2000), respectively.

	Iα					Iβ			Iγ		III		
Pressure (GPa)	0.0001	0.0001	0.0001	0.0001	0.0001	0.15 (5)	0.30 (5)	1.10 (5)	1.50 (5)		0.20 (5)	0.30 (5)	0.50 (5)
Temperature (K)	130	213	224	243	274	296 (2)	296 (2)	296 (2)	296 (2)		296 (2)	296 (2)	296 (2)
N—H1	0.88	0.86	0.96	0.96	0.97	0.97	0.92	0.89	0.88	0.89	0.96	0.95	0.95
N—H2	0.89	0.87	0.91	0.91	0.91	0.91	0.90	0.90	0.91	0.90	0.94	0.93	0.93
N···N^{i}	3.208	3.222	3.226 (1)	3.223 (1)	3.244 (2)	3.250 (6)	2.95 (1)	2.886 (9)	2.81 (1)	3.02 (4)	3.30 (2)	3.31 (3)	3.254 (4)
N···N^{ii}	3.208	3.222	3.226 (1)	3.223 (1)	3.244 (2)	3.250 (6)	2.95 (1)	2.886 (9)	2.81 (1)	3.04 (2)	3.30 (2)	3.31 (3)	3.254 (4)
N···N^{iii}	3.421	3.423	3.454 (2)	3.453 (2)	3.477 (2)	3.45 (1)	3.23 (4)	3.14 (3)	3.02 (3)	3.04 (2)	3.68 (3)	3.604 (3)	3.620 (6)
N···N^{iv}	3.762	3.794	3.782 (2)	3.784 (2)	3.809 (3)	3.80 (1)	4.50 (2)	4.36 (2)	4.17 (3)	4.17 (3)	3.68 (3)	3.604 (3)	3.620 (6)
N···N^{v}	3.822	3.829	3.843 (1)	3.847 (1)	3.868 (1)	3.866 (5)	4.50 (2)	4.36 (2)	4.52 (3)	4.52 (3)	3.66 (3)	3.64 (3)	3.615 (6)
N···N^{vi}	3.822	3.829	3.843 (1)	3.847 (1)	3.868 (1)	3.866 (5)	4.67 (3)	4.62 (3)	4.62 (4)	4.62 (3)	4.26 (1)	4.15 (3)	4.114 (7)
N···N^{vii}	4.892	4.922	4.923 (2)	4.925 (2)	4.954 (2)	4.937 (9)	4.67 (3)	4.65 (2)	4.62 (4)	4.63 (5)	4.37 (3)	4.26 (4)	4.300 (6)
N···H^{i}	3.68	3.80	3.69	3.82	3.66	3.79	3.46	3.39	2.30	3.65	3.37	3.66	3.59
N···H^{ii}	3.76	3.75	3.78	3.35	3.82	3.76	2.85	3.04	3.53	3.05	3.70	3.52	3.53
	2.34	2.37	3.78	2.28	3.80	3.74	2.15	2.04	2.69	3.75	3.70	3.73	3.66
	3.68	3.59	2.33	3.73	2.35	2.35	3.61	3.46	2.34	3.88	2.38	2.42	2.35
N···H^{iii}	4.19	4.20	2.84	4.29	2.84	2.91	3.67	3.69	3.88	4.24	4.51	4.54	4.54
	2.90	3.00	4.25	2.87	4.27	4.26	2.43	2.29	4.76	2.93	3.69	3.61	3.58
N···H^{iv}	3.38	3.43	3.33	3.38	3.38	3.27	4.57	4.51	4.79	3.60	2.81	2.67	2.70
	3.29	3.24	3.40	3.35	3.41	3.48	4.14	3.78	5.35	3.87	4.03	3.96	4.01
N···H^{v}	4.18	4.19	2.95	4.25	2.99	2.95	3.84	3.74	6.16	5.36	3.15	3.08	3.02
	2.97	3.01	4.22	3.00	4.23	4.30	4.71	4.64	5.15	4.10	3.21	3.16	3.19
N···H^{vi}	3.46	3.52	4.42	3.46	4.40	4.46	5.38	4.22	5.26	5.24	3.50	3.59	3.53
	4.39	4.34	3.46	4.40	3.51	3.44	4.74	4.42	5.06	3.81	4.79	4.52	4.57
N···H^{vii}	4.82	4.93	4.71	4.85	4.69	4.77	4.78	5.29	3.86	3.09	4.48	4.30	4.37
	4.75	4.76	4.85	4.73	4.89	4.87	5.24	4.69	5.18	4.35	5.30	5.19	5.23

Symmetry codes for phase Iα: (i) $x, \frac{1}{2}-y, z-\frac{1}{2}$; (ii) $x, \frac{1}{2}-y, z+\frac{1}{2}$; (iii) $2-x, 1-y, 1-z$; (iv) $2-x, 1-y, -z$; (v) $2-x, y-\frac{1}{2}, \frac{1}{2}-z$; (vi) $2-x, y+\frac{1}{2}, \frac{1}{2}-z$; (vii) $x-1, \frac{1}{2}-y, z-\frac{1}{2}$. Symmetry codes for phase Iβ: (i) $x, \frac{1}{2}-y, z-\frac{1}{2}$; (ii) $x, \frac{1}{2}-y, z+\frac{1}{2}$; (iii) $2-x, 1-y, 1-z$; (iv) $2-x, y-\frac{1}{2}, \frac{1}{2}-z$; (v) $2-x, y+\frac{1}{2}, \frac{1}{2}-z$; (vi) $2-x, 1-y, -z$; (vii) $1-x, y-\frac{1}{2}, \frac{1}{2}-z$. Symmetry codes for phase Iγ molecule (*a*): (i) $x, \frac{1}{2}-y, z-\frac{1}{2}$; (ii) $x, \frac{1}{2}-y, z+\frac{1}{2}$; (iii) $1-x, 1-y, 1-z$; (iv) $1-x, y-\frac{1}{2}, \frac{1}{2}-z$; (v) $1-x, y+\frac{1}{2}, \frac{1}{2}-z$; (vi) $-x, \frac{1}{2}-y, \frac{1}{2}-z$; (vii) $-x, \frac{1}{2}+y, \frac{1}{2}-z$. Symmetry codes for phase Iγ molecule (*b*): (i) $1-x, 1-y, 1-z$; (ii) $x, \frac{1}{2}-y, z-\frac{1}{2}$; (iii) $x, \frac{1}{2}-y, z+\frac{1}{2}$; (iv) $1-x, y+\frac{1}{2}, \frac{1}{2}-z$; (v) $2-x, 1-y, -z$; (vi) $1-x, 1-y, -z$; (vii) $2-x, 1-y, -z$. Symmetry codes for phase III: (i) $2-x, \frac{1}{2}-y, \frac{3}{2}-z$; (ii) $2-x, \frac{1}{2}+y, \frac{3}{2}-z$; (iii) $x, \frac{3}{2}-y, z-\frac{1}{2}$; (iv) $x, \frac{3}{2}-y, z+\frac{1}{2}$; (v) $2-x, 1-y, 1-z$; (vi) $2-x, 2-y, 1-z$; (vii)$1-x, 2-y, 1-z$.

prepared using the *X-SEED* interface of *POV-Ray* (Barbour, 2001; Persistence of Vision, 2004).

3. Results

3.1. Crystal phases and phase transitions

Five distinct phases have been distinguished out of all the diffraction studies of 1,2-diaminoethane: one study by Jamet-Delcroix (1973), one study by Thalladi *et al.* (2000) and those reported here. As already explained in §1, the structures at 213 K (Jamet-Delcroix, 1973) and at 130 K (Thalladi *et al.*, 2000) are of the same phase, denoted phase Iα. When cooled below 189 K at 0.1 MPa, phase Iα transforms to phase II – it is a first-order phase transition and phase Iα can be supercooled to 130 K. When phase Iα is pressurized to 0.2 GPa, it transforms to a similar phase, Iβ, which in turn at about 1.3 GPa changes into phase Iγ by doubling the unit-cell parameter along the crystal direction [**x**]: $a_{I\gamma} \cong 2a_{I\beta}$. Phase III has not been observed at atmospheric pressure and it appears to be stable only above 0.15 GPa. These experimental data from X-ray and thermal analyses, as well as the analyses of crystal structures, allow new features of the phase diagram of 1,2-diaminoethane to be outlined, as shown in Fig. 7.

The pressure dependence of the unit-cell dimensions shown in Figs. 5 and 6 demonstrates clearly that 1,2-diaminoethane crystals in phase Iα, which were previously obtained by temperature freezing (Jamet-Delcroix, 1973; Thalladi *et al.*, 2000), are also stabilized by pressure at 296 K. Above 0.15 GPa the unit-cell dimensions of phase Iα abruptly change, but the crystal preserves the $P2_1/c$ space-group symmetry. This transformation of unit-cell parameters is accompanied by a change of molecular volume (Fig. 4) and structural changes (discussed below), all of which indicate that the crystal undergoes an isostructural phase transition to phase Iβ. The crystal compression is comparable to those of other molecular compounds (Boldyreva *et al.*, 2004). At still higher pressure, between 1.1 and 1.5 GPa, the $a_{I\beta}$ parameter of the unit-cell doubles (new weak reflections have been observed) which suggests another, probably continuous, transition to phase Iγ. The pressure dependence of the unit-cell dimensions of phases Iα, Iβ and Iγ suggests that their structures are related and that differences between these phases are not drastic. For this reason labels Iα, Iβ and Iγ have been assigned to indicate the structure relations between these phases.

It can be seen from Fig. 5 that the unit-cell dimensions of phase III are considerably different from those of phase I, and it can be inferred that its structure is also very different. The temperature dependence of the unit-cell dimensions shows that phase Iα obtained by temperature-freezing is stable down to 189 K, at which point it undergoes a strong first-order phase transition. This conclusion is strongly corroborated by a considerable hysteresis, as shown by the structural determination of 1,2-diaminoethane in phase Iα at 130 K (Thalladi *et*

al., 2000), *i.e.* 59° below the phase-transition temperature determined by Messerly *et al.* (1975). This 1,2-diaminoethane phase, stable at 0.1 MPa below 189 K, was denoted as phase II. This phase II is different from phases Iβ or Iγ, because structural changes between phases Iα and Iβ or Iγ are too subtle to cause the crystal shattering reported by Jamet-Delcroix (1973) and observed by us. The existence of phase II has been also shown by the powder-diffraction data described in §2.

3.2. Structures of phases Iα, Iβ and Iγ

Phases Iα, Iβ and Iγ of 1,2-diaminoethane are all monoclinic, space group $P2_1/c$, with half of the molecule symmetry-independent in phases Iα and Iβ, and two halves of the molecule symmetry independent in phase Iγ. In all these structures the molecules are located on inversion centres.

The shortest intermolecular contacts involve the amino groups. These interactions can be described as weak or very weak hydrogen bonds. The two shortest hydrogen bonds link the molecules into sheets in the crystal structures of phases Iα, Iβ (Figs. 8 and 9) and Iγ. The shortest N···N distances in the 1,2-diaminoethane phases are listed in Table 3. In the phase Iα structures, all determined at 0.1 MPa except for one at 0.15 GPa, there are two shortest N···N contacts of *ca* 3.20 Å and a longer one of *ca* 3.50 Å. At 0.3 GPa the two shorter of these contacts are squeezed by *ca* 0.25 Å and the longer one is squeezed by 0.2 Å. These changes are plotted in Fig. 10, where all N···N distances shorter than 5 Å have been included for a more complete illustration of the structural changes at the phase transitions. It can be seen that somewhat longer N···N distances, three of which are of about 3.8 Å in phase Iα, also abruptly change, but they expand by about 0.7 Å between 0.15 and 0.3 GPa. The anomalous pressure dependence of N···N distances corroborates the observation of discontinuities in the crystal compression and is the main argument for distinguishing phases Iα and Iβ.

3.3. Structure of phase III

The 1,2-diaminoethane crystal in phase III is monoclinic, space group $P2_1/c$, with half of the molecule symmetry independent. As in phases Iα, Iβ and Iγ the molecules are located on inversion centres. The molecular packing in phase III is shown in Fig. 11.

The main differences between phases I and III are in the unit-cell dimensions, described in §3.1, and in the orientation

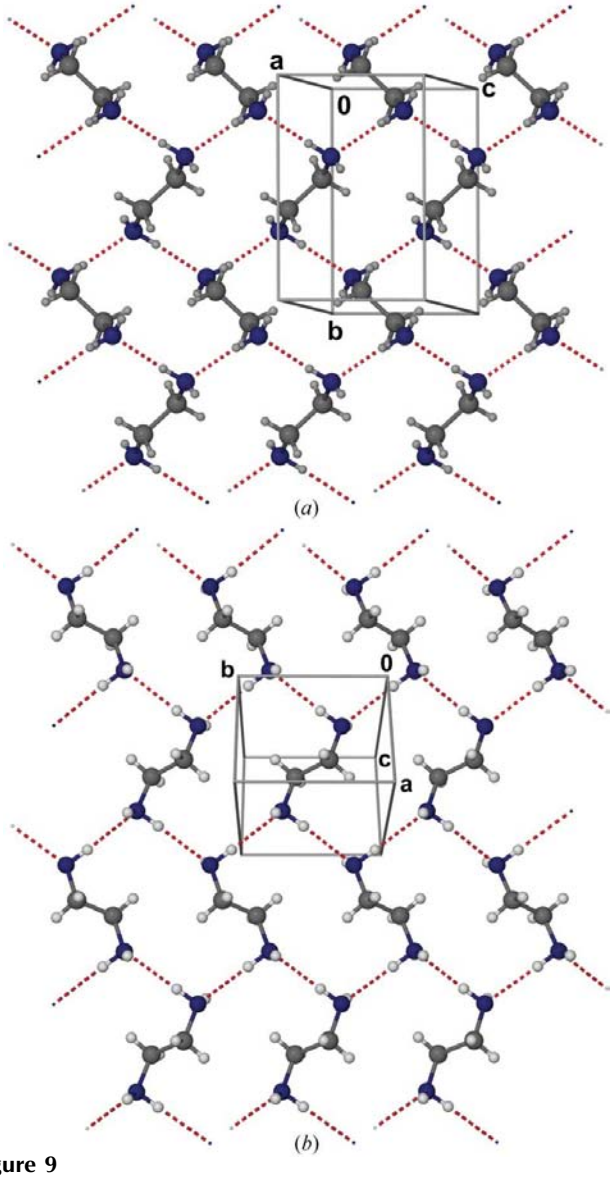

Figure 9
Autostereographic (Katrusiak, 2001) projections of layers formed by the two shortest hydrogen bonds (per one –NH_2 group) in 1,2-diaminoethane structures: (*a*) in phase Iβ at 1.1 GPa/296 K and (*b*) in phase III at 0.2 GPa/296 K. In addition to the two shortest NH···N bonds forming the layers, the NH···N bonds extending to neighbouring layers are also shown. The hydrogen bonds are indicated with red dashed lines.

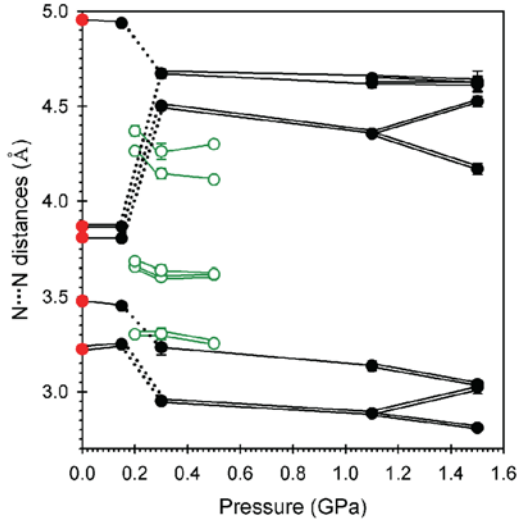

Figure 10
The pressure dependence of N···N distances in phases Iα, Iβ, Iγ (black circles) and III (green empty circles) at 296 K. Red points at 0.1 MPa refer to 274 K. For all plotted data, except one point in the structure at 1.5 GPa, the error bars are smaller than the size of the symbol. Close parallel lines have been used to indicate the presence of two identical N···N distances (see Table 3).

Table 4
The τ_e angles observed in the low-temperature and high-pressure structures of 1,2-diaminoethane.

	Iα				Iβ		Iγ		III		
Pressure (GPa)	0.0001	0.0001	0.0001	0.15	0.3	1.1	1.5	–	0.2	0.3	0.5
Temperature (K)	224	243	274	296	296	296	296	–	296	296	296
τ_e (°)	179.9	179.6	177.4	−176.3	164.7	179.4	99.1	135.5	179.5	−174.4	−175.0

Table 5
The intermolecular C—N···N^i—C^i torsion angles about the shortest NH···N hydrogen bonds for each amino group in structures of 1,2-diaminoethane phases.

Two symmetry-independent values are given for phase Iγ.

	Iα				Iβ		Iγ		III		
Pressure (GPa)	0.0001	0.0001	0.0001	0.15	0.3	1.1	1.5	–	0.2	0.3	0.5
Temperature (K)	224	243	274	296	296	296	296	–	296	296	296
C—N···N^i—C^i	31.45	31.47	31.80	31.99	46.18	41.46	48.20	176.99	159.56	157.64	158.84
	(0.12)	(0.10)	(0.18)	(0.39)	(1.81)	(0.97)	(2.56)	(2.20)	(0.73)	(1.26)	(0.29)

Symmetry codes: for phases Iα, Iβ and for the first molecules in phase Iγ: (i) $x, \frac{1}{2}-y, z-\frac{1}{2}$; the second molecule in phase Iγ: (i) $1-x, 1-y, 1-z$; for phase III: (i) $2-x, \frac{1}{2}-y, \frac{3}{2}-z$.

of interacting molecules. The two shortest N···N distances in phase III are comparable in length to the two shortest N···N contacts in phase Iα, whereas there are three next shortest N···N contacts of similar length in phase III, which are considerably longer than the third shortest N···N distance in phase Iα (see Fig. 10 and Table 3).

3.4. Hydrogen bonding in phases I and phase III

The molecular association in the crystal structures of 1,2-diaminoethane is clearly governed by the formation of weak NH···N hydrogen bonds (albeit much stronger in phase Iβ than in phases Iα and III). The hydrogen-bonding geometry in phases Iα, Iβ and III is different. The longer N···N distances in phases Iα and III can be explained by the dynamical rotations of the NH_2 groups about the C—N bonds. The presence of two N···N contacts somewhat shorter (by more than 0.2 Å) than other the N···N contacts in each of these structures is a common feature of phases I and III. The crystal structures of 1,2-diaminoethane phases can thus be considered as built of layers where each molecule is NH···N bonded to its four neighbours. These layers, shown in Fig. 9, are considerably different in phases I and III, even though the pattern of the hydrogen bonding is identical (Etter, 1990; Etter *et al.*, 1990; Grell *et al.*, 1999); the layers differ by the orientation of the molecules relative to the layer direction. The dimensions of hydrogen bonds and the shortest interatomic distances are listed in Table 3.

4. Discussion

4.1. Molecular conformation

The conformations of the 1,2-diaminoethane molecule can be described, analogously to the ethylene glycol molecule (Howard *et al.*, 2005), by three descriptors: (i) a lower-case-letter acronym of *gauche*$^+$, *gauche*$^-$ or *trans* conformations describing the N-atom electron lone-pair torsion angle with respect to the C—C bond, (ii) a capital-letter acronym describing the N—C—C—N torsion angle, and (iii) a lower-case-letter acronym describing the torsion angle of the other electron lone pair. The torsion angle describing a conformation of the N lone electron pair (τ_e) can be readily calculated from the H1—N—C—C (τ_{H1}) and H2—N—C—C (τ_{H2}) torsion angles, according to the equation

$$\tau_e = (\tau_{H1} + \tau_{H2})/2 \pm 180^\circ, \qquad (2)$$

the final operator in the summation being chosen as that which gives the smaller absolute value of the result. The observed τ_e conformations are listed in Table 4.

It is striking that all molecules in all 1,2-diaminoethane phases have the *tTt* conformation, except phase Iγ, in which the a^+Ta^- conformation occurs, where *a* is the acronym of the anticlinal conformation (McNaught & Wilkinson, 1997). Thus, the differences in the 1,2-diaminoethane structures involve mainly transformations of hydrogen bonds and rearrangements of the molecules. For example, the C—N···N^i—C^i angles between hydrogen-bonded molecules are considerably different in phases Iα, Iβ, Iγ and III (Table 5).

4.2. Hydrogen bonding in 1,2-diaminoethane

The formation of the NH···N bonds in 1,2-diaminoethane structures depends on the orientation of the close $-NH_2$ groups. The polymorphs of 1,2-diaminoethane present a

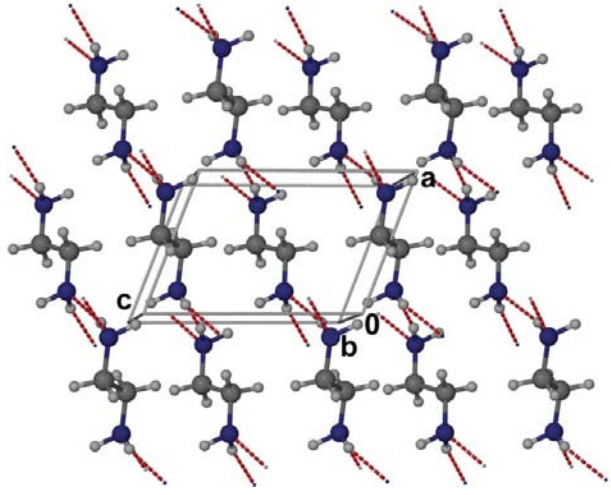

Figure 11
Autostereogram of molecular packing in phase III of 1,2-diaminoethane at 0.2 GPa/296 K, with the closest N···H contacts indicated as red dashed lines. The NH···N-bonded sheets, one of which is shown in Fig. 9, run along the crystal $(10\bar{2})$ planes, perpendicular to this drawing.

model situation, where the NH···N bonds are relatively weak and can be formed and broken following amino-group rotations. The closest of the N···N contacts range from 2.811 Å (form Iγ at 1.5 GPa) to 3.302 Å (form III at 0.2 GPa) and 3.223 Å (form Iα at 243 K). This criterion of the three shortest intermolecular N···N distances has been used below to consider the hydrogen-bond character of interacting amino groups. If only the two shortest NH···N bonds were considered only, the patterns of hydrogen bonds in phases Iα, Iβ and III would be the same: sheets of NH···N-bonded molecules formed from $C(2)$ and $C(5)$ chains and $R_4^4(14)$ rings (Fig. 10). However, in phase III, the difference between the third, fourth and fifth shortest N···N distances is only marginal; the two shortest N···N distances in phase III are identical and symmetry-related, and two of the next shortest N···N distances are also identical (Table 3).

The observed relations between the NH···N bonds and other contacts of amino groups can be rationalized by rotations of the NH_2 groups about N—C bonds. These rotations can be damped by high pressure or low temperature. Four hydrogen-bond donors and two acceptors per molecule can form four intermolecular NH···N hydrogen bonds in the 1,2-diaminoethane structures. Thus, of one amino group only one H atom and the one electron pair can be involved in a stable hydrogen bond, while for the second H atom there would be no acceptor left to form an NH···N interaction. The hydrogen-bonding scheme of the stable (*i.e.* not rotating) amino groups is illustrated in Fig. 12(*a*). It is also possible that the NH_2 groups rotate such that the time-averaged occupancy of the H atoms in each of three sites is equal to 2/3, as shown in Fig. 12(*c*). Another disorder model allows NH_2 group rotations by $\pm120^\circ$, such that the H-atom site occupancy in one direction is equal to 1.0 and that in the other two directions is 0.5, as illustrated in Fig. 12(*b*). In the three models presented above only two (Fig. 12*a*) or three (Figs. 12*b* and 12*c*) H-atom sites are permitted. The assumption of three H-atom sites is justified by the existence of hydrogen bonds and also by conformational preferences of the 1,2-diaminoethane molecule.

The three models of the NH_2 group disorder lead to different occupancies of the H-atom sites that are essential for the intermolecular interactions. For the purpose of this discussion we will consider only the equilibrated configurations of hydrogen bonds relevant to the crystal structure (*i.e.* excluding H-glasses, multi-configurational states and their fluctuations). Thus, in the ordered model (Fig. 12*a*), the NH_2 group can form two hydrogen bonds; this NH_2 group serves as an H-atom donor for one of these hydrogen bonds and as an acceptor for the other. The second H atom, because of the deficiency of H-atom acceptors, would form van der Waals contacts only. An analogous situation, of the NH_2 group forming two hydrogen bonds, would be observed for the NH_2 group restricted to $\pm120^\circ$ rotations (Fig. 12*c*). In both these models, either the ordered H atoms or restricted rotations of the amine groups, there would be one H atom per hydrogen bond and two H atoms per van der Waals contact, if we assume that each NH_2 group interacts with three amino groups distributed at about 120° intervals about it. The unrestricted rotations (Fig. 12*c*) would lead to the equal time-averaged distribution of 4/3 H atoms for each of three contacts of amino groups. Naturally, apart from these three $-NH_2$ group disorder models, intermediate types of disorder are also possible.

At room temperature the rotations of the amino groups in 1,2-diaminoethane are activated (Williams *et al.*, 1990; Michalczyk & Russu, 1999), and therefore at high temperature 1,2-diaminoethane is likely to freeze in the structure imposing no hindrances for the amino-group rotations. The NH_2 groups are likely to rotate in the structure frozen by cooling, because 1,2-diaminoethane freezes at relatively high temperature (284 K), and in the structure obtained by pressure freezing, because the freezing pressure of 0.15 GPa at 296 K is relatively low. It can be observed from Fig. 10 that there is more space around amino N atoms in phase III at 0.2 GPa than in phase Iα at 0.1 MPa. When subjected to a pressure of 0.2 GPa phase Iα transforms to phase Iβ, and the molecules shift slightly such that two NH···N hydrogen bonds become shorter and stronger. The non-continuous change of N···N distances *versus* pressure is clearly visible in Fig. 10. It is plausible, that the NH_2-group behaviour in phase Iα is intermediate between the models presented in Fig. 12, and that at 0.2 GPa one of these components (for example, the unrestricted rotation) is eliminated.

Because phase III crystallizes at room temperature, unrestricted NH_2-group rotations are more likely in its structure than in that of phase Iα frozen at low temperatures,

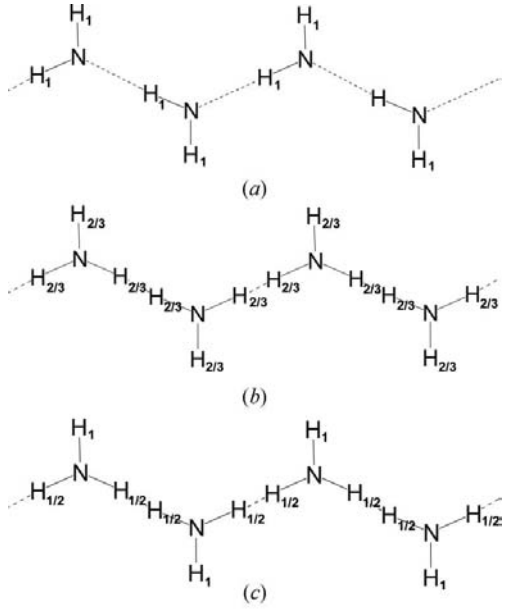

Figure 12
The ordered and rotationally disordered NH_2 groups in the hydrogen-bonded 1,2-diaminoethane aggregate: (*a*) the ordered hydrogen-bonded NH_2 groups (the N—C bonds have been omitted), when the molecular conformation does not change and the two H-atom sites have full occupancy; (*b*) the partly disordered H atoms as a result of $\pm120^\circ$ rotations of NH_2 groups resulting in two sites with 1/2 occupancy and one site with full occupancy; (*c*) three H-atom sites with 2/3 occupancy as a result of the unrestricted rotations of NH_2 groups about the C—N bonds.

when activation of the NH_2 rotations is more difficult and less likely. Thus the model of restricted ($\pm 120^\circ$) NH_2 rotations is more likely for freezing by cooling than by pressurizing. The restricted NH_2 rotations are still very favourable for the formation of two NH···N bonds, as explained above, whereas the full rotations require more space around the NH_2 groups. Above 0.2 GPa phase Iα transforms into the Iβ structure with stronger hydrogen bonding, whereas the compression of phase III is monotonic. Thus, it is plausible that the Iα-to-Iβ transition is caused by damping of the NH_2-group rotations. In phase III this process is probably distributed over a longer pressure range, as a result of the larger voids about the NH_2 groups.

5. Separation of phases

We have attempted to cocrystallize 1,2-diaminoethane with 1,2-dihydroxyethane, $C_2H_6O_2$ (m.p. 260.46 K (Ott *et al.*, 1972), by pressure freezing. There is an excess of four hydrogen-bond acceptors over two donors in the 1,2-dihydroxyethane molecule, the reverse of the situation in 1,2-diaminoethane, and it was intended to check if the precise match of H-atom donors and acceptors in a 1:1 mixture of these compounds would result in a stable structure of OH···N- and NH···O-bonded molecules. The molecular structures of these two compounds are also very similar, and their molecular weights are nearly identical. However, the phases separated and at 0.15 GPa the 1,2-diaminoethane crystal started to grow in 1,2-dihydroxyethane (still liquid at 0.15 GPa). It appears that this separation may be caused by the conformational properties, which are very different for the 1,2-diaminoethane and 1,2-dihydroxyethane molecules (Budzianowski & Katrusiak, 2006*b*).

6. Conclusions

The determinations of low-temperature and high-pressure structures of 1,2-diaminoethane revealed new phases and phase transitions of this compound, which can be rationalized in terms of NH_2-group rotations and transformations of the NH···N-bonding contacts. In this respect, 1,2-diaminoethane can be considered as an ice-structure analogue, where the hydrogen-bonded groups rotate. It is plausible that the NH_2-group rotations in conjunction with the excess of H-atom donor groups in 1,2-diaminoethane result in the amino H-atom ordering and abrupt transformations between phases Iα and Iβ. In all 1,2-diaminoethane phases the molecular N—C—C—N torsion angle is identical and equal to 180° and the average H—N—C—C torsion angles correspond to a *gauche* conformations. Thus, despite the NH_2-group rotation, the 1,2-diaminoethane molecules exhibit a consistent average conformation, *tTt*, in all the crystalline phases. Of the five known phases of 1,2-diaminoethane, the structure of phase II is still unknown, and should be determined for a better understanding of the properties of this interesting compound. A powder diffraction study of phase II is in progress. Despite having apparently analogous structures and a compensating number of hydrogen-bond donors and acceptors, the 1:1 1,2-diaminoethane:1,2-dihydroxyethane mixture separates at 0.15 GPa.

This study was supported by the Polish Ministry of Scientific Research and Information Technology, grant No. 3T09A18127.

References

Barbour, L. J. (2001). *J. Supramol. Chem.* **1**, 189–191.

Boldyreva, E. V., Drebushchak, T. N., Shakhtshneider, T. P., Sowa, H., Ahsbahs, H., Goryainow, S. V., Ivashevskaya, S. N., Kolesnik, E. N., Drebushchak, V. A. & Burgina, E. B. (2004). *ARKIVOC*, (XII), 128–155.

Budzianowski, A. & Katrusiak, A. (2004). *High-Pressure Crystallographic Experiments with a CCD Detector* in *High-Pressure Crystallography*, edited by A. Katrusiak & P. F. McMillan, pp. 157–168. Dordrecht: Kluwer Academic Publisher.

Budzianowski, A. & Katrusiak, A. (2006*a*). *J. Phys. Chem. B*, **110**, 9755–9758.

Budzianowski, A. & Katrusiak, A. (2006*b*). In preparation.

Etter, M. C. (1990). *Acc. Chem. Res.* **23**, 120–126.

Etter, M. C., MacDonald, J. C. & Bernstein, J. (1990). *Acta Cryst.* B**46**, 256–262.

Grell, J., Bernstein, J. & Tinhofer, G. (1999). *Acta Cryst.* B**55**, 1030–1043.

Howard, D. L., Jörgensen, P. & Kjaergaard, H. G. (2005). *J. Am. Chem. Soc.* **127**, 17096–17103.

Jamet-Delcroix, S. (1973). *Acta Cryst.* B**29**, 977–980.

Katrusiak, A. (2001). *J. Mol. Graph. Model.* **19**, 363–367, 398.

Katrusiak, A. (2003). *REDSHAD*. Adam Mickiewicz University, Poznań, Poland.

Katrusiak, A. (2004). *Z. Kristallogr.* **219**, 461–467.

Katrusiak, A. (2006). In preparation.

Katrusiak, A. & Szafrański, M. (1999). *Phys. Rev. Lett.* **82**, 576–579.

McNaught, A. D. & Wilkinson, A. (1997). *Compendium of Chemical Terminology, The Gold Book*, 2nd ed. Cambridge, UK: Blackwell Science.

Mao, H. K., Xu, J. & Bell, P. M. (1985). *J. Geophys. Res.* **91**, 4673–4676.

Messerly, J. F., Finke, H. Z., Osborn, A. G. & Douslin, D. R. (1975). *J. Chem. Thermodyn.* **7**, 1029–1046.

Michalczyk, R. & Russu, I. M. (1999). *Biophys. J.* **76**, 2679–2686.

Ott, J. B., Goates, J. R. & Lamb, J. D. (1972). *J. Chem. Thermodyn.* **4**, 123–126.

Oxford Diffraction (2002). *Xcalibur Series Single-Crystal Diffractometers, User Manual*, Version 1.3. Oxford Diffraction Poland, Wrocław, Poland.

Persistence of Vision (2004). *Raytracer*, Version 2.6. Persistence of Vision Pty. Ltd, Williamstown, Victoria, Australia.

Piermarini, G. J., Block, S., Barnett, J. D. & Forman, R. A. (1975). *J. Appl. Phys.* **46**, 2774–2780.

Sheldrick, G. M. (1990). *Acta Cryst.* A**46**, 467–473.

Sheldrick, G. M. (1997). *The SHELX97 Manual.* University of Göttingen, Germany.

Sigma–Aldrich (2005). *Aldrich Advancing Science 2005–2006 Poland*, p. 805. Sigma–Aldrich Corporation, Poznan, Poland.

Szafrański, M. & Katrusiak, A. (2004). *J. Phys. Chem.* **108**, 15709–15713.

Szafrański, M., Katrusiak, A. & McIntyre, G. J. (2002). *Phys. Rev. Lett.* **89**, 215507.

Thalladi, V. R., Boese, R. & Weiss, H. Ch. (2000). *Angew. Chem. Int. Ed.* **39**, 918–922.

Williams, L. D. & Williams, N. G. & Shaw, B. R. (1990). *J. Am. Chem. Soc.* **112**, 829–833.

Wilson, L. C., Wilson, H. L., Wilding, W. V. & Wilson, G. M. (1996). *J. Chem. Eng. Data*, **41**, 1252–1254.